Journal of Experimental Botany, Vol. 70, No. 4 pp. 1283–1297, 2019
doi:10.1093/jxb/ery443 Advance Access Publication 21 December 2018
This paper is available online free of all access charges (see https://academic.oup.com/jxb/pages/openaccess for further details)

RESEARCH PAPER

Rubisco carboxylation kinetics and inorganic carbon utilization in polar versus cold-temperate seaweeds

Concepción Iñiguez[1,2,*], Jeroni Galmés[2], and Francisco J. L. Gordillo[1]

[1] Department of Ecology, Faculty of Sciences, University of Malaga, Boulevard Louis Pasteur s/n, 29010 Málaga, Spain
[2] Research Group in Plant Biology under Mediterranean Conditions, Universitat de les Illes Balears-INAGEA, Carretera de Valldemossa km 7.5, 07122 Palma, Illes Balears, Spain

* Correspondence: iniguez@uma.es

Received 16 August 2018; Editorial decision 6 December 2018; Accepted 7 December 2018

Editor: Howard Griffiths, University of Cambridge, UK

Abstract

Despite the high productivity and ecological importance of seaweeds in polar coastal regions, little is known about their carbon utilization mechanisms, especially the kinetics of the CO_2-fixing enzyme Rubisco. We analyzed Rubisco carboxylation kinetics at 4 °C and 25 °C in 12 diverse polar seaweed species (including cold-temperate populations of the same species) and the relationship with their ability to use bicarbonate, by using ^{13}C isotope discrimination and pH drift experiments. We observed a large variation in Rubisco carboxylation kinetics among the selected species, although no correlation was found between either the Michaelis–Menten constant for CO_2 (K_c) or Rubisco content per total soluble protein ([Rubisco]/[TSP]) and the ability to use bicarbonate for non-green seaweeds. This study reports intraspecific Rubisco cold adaptation by means of either higher Rubisco carboxylation turnover rate (k_{cat}^c) and carboxylase efficiency (k_{cat}^c/K_c) at 4 °C or higher [Rubisco]/[TSP] in some of the analyzed species. Our data point to a widespread ability for photosynthetic bicarbonate usage among polar seaweeds, despite the higher affinity of Rubisco for CO_2 and higher dissolved CO_2 concentration in cold seawater. Moreover, the reported catalytic variation within form ID Rubisco might avert the canonical trade-off previously observed between K_c and k_{cat}^c for plant Rubiscos.

Keywords: Carbon concentrating mechanisms, carbon fixation, kinetics, macroalgae, photosynthesis, polar, Rubisco, seaweeds.

Introduction

Littoral and sublittoral hardbottom zones of polar coastal regions are mainly dominated by dense macroalgal communities, which represent a major trophic contribution to these ecosystems (Dunton and Schell, 1987; Amsler *et al.*, 1995; Iken *et al.*, 1998). The productivity of these communities is comparable to that of temperate seaweed forests (Quartino and Boraso de Zaixso, 2008; Hop *et al.*, 2012), despite the low temperatures in polar regions. Thus, polar seaweeds may have developed photosynthetic adaptations to cold waters, although little is known about the specific molecular processes involved in inorganic carbon (C_i) acquisition and assimilation in these organisms.

The first major step of photosynthetic carbon fixation is catalyzed by the enzyme ribulose-1,5-bisphosphate carboxylase oxygenase (Rubisco, EC 4.1.1.39). Rubisco is present in most autotrophic organisms from prokaryotes, such as photosynthetic anaerobic bacteria and cyanobacteria, to eukaryotes, such as algae and higher plants (Whitney *et al.*, 2011). Almost

all O_2 evolvers have a form I Rubisco, which consists of eight large and eight small subunits and is subdivided into forms IA–ID depending on its sequence and lineage (Tabita *et al.*, 2008). Plants, green algae, and most cyanobacteria belong to the 'green' chloroplast lineage possessing form IB Rubiscos, while non-green algae from the 'red' chloroplast lineage contain form ID Rubiscos (Raven and Beardall, 2003; Falkowski *et al.*, 2004).

In spite of their relevance in global carbon cycling, all Rubiscos have a relatively slow carboxylation turnover rate (k_{cat}^c) and low affinity for CO_2, along with poor discrimination between CO_2 and O_2 (Spreitzer and Salvucci, 2002). These catalytic traits, together with the low levels of dissolved CO_2 and slow CO_2 diffusion rate in water, have led to the evolution of carbon concentrating mechanisms (CCMs) in most aquatic photosynthetic organisms (Giordano *et al.*, 2005). CCMs consist of an active influx of CO_2 and/or HCO_3^- at the plasmalemma and/or a plastid envelope membrane, which act to increase the CO_2 concentration around Rubisco (Maberly *et al.*, 1992; Raven and Beardall, 2003; Giordano *et al.*, 2005). Only a few seaweed species appear to lack CCMs (in these species, photosynthesis relies only on passive diffusion of CO_2), although in many cases stronger evidence on the presence or absence of CCMs is required (Raven *et al.*, 2005).

Different physiological measurements have been widely used to suggest the presence or absence of CCMs; these include the pH compensation point, the activity of transporters or enzymes that are part of a CCM, and the natural $^{13}C/^{12}C$ ratio in the algal biomass, among others. The ^{13}C isotope discrimination of the algal biomass ($\delta^{13}C_{alga}$), relative to the isotope composition of the C_i source, is primarily controlled by the interplay between C_i supply and demand, which affects CO_2/HCO_3^- acquisition and accumulation (i.e. CCMs), as well as CO_2 fixation and CO_2 leakage out of the cell (Sharkey and Berry, 1985). It has been frequently used as a proxy for CCM operation in seaweeds, assuming low leakage, since the increase in the utilization of isotopically heavier HCO_3^- relative to isotopically lighter CO_2 produces a decrease in the ^{13}C isotope discrimination of the algal biomass (higher $\delta^{13}C_{alga}$) with respect to the isotope fractionation of Rubisco (Raven *et al.*, 2002*a*). The pH compensation point indicates the condition in which the dissolved inorganic carbon (DIC) taken up by the alga equals the CO_2 released into the medium by respiration and/or photorespiration. Maberly *et al.* (1992) reported $\delta^{13}C_{alga}$ values more negative than or equal to –30‰ for all seaweeds showing pH compensation points lower than 9.0, that is, the pH at which the dissolved CO_2 concentration is nearly zero. Since the ratio of the Rubisco reaction rate with $^{12}CO_2$ to that with $^{13}CO_2$ is 1.030 (at least for spinach Rubisco, Roeske and O'Leary, 1984; see Boller *et al.*, 2015 for other Rubisco types), both measurements suggest that photosynthesis in these seaweeds might rely only on diffusive CO_2 entry. These species are mainly red algae from the class Florideophyceae inhabiting subtidal habitats, where light is presumed to be the limiting resource (Maberly *et al.*, 1992; Raven *et al.*, 2002*a*).

While the production and operation of CCMs are energy- and resource-demanding processes, diffusive entry of CO_2 for photosynthesis at the current CO_2 levels may allow significant oxygenase activity of Rubisco, thereby decreasing the efficiency of photosynthesis; in addition, the photorespiratory metabolism also has an associated energetic cost that depends on the Rubisco CO_2/O_2 specificity factor ($S_{C/O}$; Raven *et al.*, 2014). Thus, Rubisco may have evolved towards an increased affinity for CO_2, that is, a decreased Michaelis–Menten affinity constant for CO_2 (K_c; Nisbet *et al.*, 2007) in those organisms relying only on diffusive entry of CO_2. In fact, in the few rhodophyte species analyzed to date, Rubisco has a high $S_{C/O}$ value (Badger *et al.*, 1998). However, most of these rhodophytes are thermo-acidophiles, which are not representative of all species belonging to this phylum. On the other hand, the evolution of CCMs has probably removed some of the pressure to enhance carboxylation efficiency (Meyer and Griffiths, 2013). In this sense, Rubisco from green algae with CCMs and cyanobacteria were found to have high K_c and k_{cat}^c (Yeoh *et al.*, 1981; Andrews and Lorimer, 1985; Mueller-Cajar and Whitney, 2008). It is still unknown whether the same applies to ID Rubiscos from non-green algae possessing CCMs. Recently, Young *et al.* (2016) have reported that Rubisco from diatoms, which have efficient CCMs, exhibits a broad range of K_c values that mostly exceed those of C_4 plant Rubisco, but similar and less variable k_{cat}^c values, suggesting that the canonical trade-off typically observed between K_c and k_{cat}^c for plant form IB Rubisco might not exist for form ID Rubisco. Nevertheless, more data are required to confirm this observation.

Raven *et al.* (2002*b*) suggested that the impact of low seawater temperatures on photosynthesis would favor diffusive CO_2 entry rather than CCM operation. The affinity for CO_2 and $S_{C/O}$ of Rubisco increase at decreasing temperatures, while the carboxylation efficiency notably decreases (k_{cat}^c/K_c; Jordan and Ogren, 1984; Perdomo *et al.*, 2015; Galmés *et al.*, 2016). It has been hypothesized that the rate of CO_2 supply to Rubisco would not change significantly at lower temperatures, since the elevated concentrations of dissolved CO_2 in cold waters mostly compensate for the lower diffusion coefficient of CO_2 (Raven *et al.*, 2002*b*); so, assuming no increase in Rubisco content at low temperatures, the reduced carboxylation efficiency would lead to a greater CO_2 concentration around Rubisco (C_c) during steady-state photosynthesis. However, the previous assumption might be altered by other factors, including changes in the activation state of the enzyme, a probable decrease in the contribution of respiratory and photorespiratory CO_2, and a larger diffusion boundary layer thickness and changes in transmembrane components affecting the conductance for CO_2.

In temperate seaweeds, the acclimation of photosynthesis to low temperature involved the production of high concentrations of Calvin cycle enzymes (Davison, 1987). Similarly, higher plants grown at low temperatures up-regulate their Rubisco content, compensating for the intrinsic decline in k_{cat}^c (Holaday *et al.*, 1992; Yamori *et al.*, 2005). This significant increase in Rubisco content might be energetically costly for cold-adapted organisms and requires a high nitrogen (N) investment. Alternatively, photosynthetic adaptation to cold environments by means of higher Rubisco k_{cat}^c values, allowing for a partial compensation of the intrinsic decline in enzymatic activity at low temperatures, would represent N and

energy savings for the organism. In this regard, Rubiscos from plants belonging to colder climates typically showed a 40% faster k_{cat}^c than warm-adapted species when both groups were measured at a standard temperature of 25–30 °C (Sage, 2002; Galmés *et al.*, 2015). Unfortunately, Rubisco kinetics have been barely examined in seaweeds, except for a few species (Yeoh *et al.*, 1981; Johnston, 1991; Whitney *et al.*, 2001; Israel and Hophy, 2002); most of these studies measured K_c at only a single temperature and none of them included polar species. Therefore, more data are needed to explore adaptation patterns in Rubisco investment, kinetics, and C_i acquisition mechanisms in seaweeds from different latitudes. This knowledge would be especially useful for the prediction of the consequences of global change in macroalgal communities at high latitudes. The aim of the present study was to identify the presence of adaptive traits in Rubisco kinetics and Rubisco content of macroalgal species representative of Arctic and Antarctic ecosystems, to compare them with populations of the same species from cold-temperate latitudes when possible, and to relate these data to the presence or absence of CCMs in these species.

Materials and methods

Algal material

Twelve different macroalgal species representative of Arctic and Antarctic ecosystems, including some populations of the same species from cold-temperate latitudes, were analyzed. The selected species included taxa with contrasting habitat ecologies and evolutionary histories (see Table 1). The analyzed polar and cold-temperate populations belonging to the same species had previously been identified as different ecotypes (Bischoff and Wiencke, 1995; Van de Poll *et al.*, 2002; Olischläger *et al.*, 2017). For some of the species, samples were collected by divers during July 2013 in Kongsfjorden, Spitsbergen, Svalbard (79°N, 11°E), or May 2015 in Helgoland, Germany (54°N, 7°E), and immediately taken to the laboratory in black plastic bags. Young (when possible) and visually healthy specimens free from macroscopic epibiota were chosen for the analyses. For the remainder of the species studied, young macrothalli were raised from the Alfred Wegener Institute (AWI, Bremerhaven, Germany) stock cultures. Cultivation methods were as described by Wiencke and tom Dieck (1989). *Saccharina latissima* from Helgoland was grown at 17±1 °C, and *Palmaria palmata* from Roscoff, *Acrosiphonia arcta* from Helgoland, and *S. latissima* from Spitsbergen were grown at 10±1 °C. These species were cultured using a 16:8 h light:dark photoperiod and a constant photon fluence rate (PFR) of 25–30 µmol photons m^{-2} s^{-1} provided by white light fluorescent tubes (Osram 58W/965 Biolux). The rest of the polar species were grown at 1±1 °C with a changing photoperiod from 5 to 20 h of light to mimic high-latitude seasonal conditions. PFR was measured by means of a quantum flat-head PAR sensor connected to a radiometer (LI-190 and LI-250A, LI-COR Biosciences). Samples for determination of relative Rubisco content, kinetic characterization, and carbon stable isotope composition were snap frozen in liquid nitrogen and stored at –80 °C until analysis.

Carbon stable isotope composition

The abundance of ^{13}C relative to ^{12}C in the algal samples was determined by mass spectrometry using a DELTA V Advantage (Thermo Electron Corporation) isotope ratio mass spectrometer (IRMS) connected to a Flash EA 1112 CNH analyzer (Thermo Electron Corporation). The calculated $\delta^{13}C_{alga}$ was corrected with the isotope composition of DIC found in the medium from which the samples were collected ($\delta^{13}C_{DIC}$), as described by Iñiguez *et al.* (2016*a*, *b*). Measurements of $\delta^{13}C_{DIC}$ were done with the same IRMS connected to a GasBench II system (Thermo Electron Corporation).

pH drift

Specimens were placed in 100 ml glass bottles completely filled with 0.2 µm-filtered seawater, with magnetic stirring, and tightly sealed to avoid gas exchange with the air. Assays were performed at saturating PFR (previously determined for each species by chlorophyll *a* fluorescence rapid light curves by means of a pulse-amplitude-modulated fluorometer; Mini-PAM, Walz) at their respective growth temperatures for specimens from stock cultures, or at 3±1 °C for the species collected in Kongsfjorden. Specimen size was adjusted to prevent self-shading and to ensure effective agitation of the medium. The pH was recorded using a thin glass electrode (CRISON 52 09, pH meter CRISON GLP 22) until it reached a stable reading (after ~24 hours of incubation), which represents the pH compensation point.

Rubisco content and carboxylase kinetics

Rubisco carboxylation kinetics (k_{cat}^c and K_c) were determined at 25 °C and 4 °C in rapid crude protein extracts, according to the methods described for plants (Sharwood *et al.*, 2008, 2016) and algae (Heureux *et al.*, 2017; Young *et al.*, 2016). Rapidly prepared fresh extracts instead of purified Rubisco preparations were used to prevent the degradation of Rubisco because the C-terminal loop of the enzyme is often a target for proteases, which results in changes in the catalytic performance (Sharwood *et al.*, 2008). Approximately 0.5 g fresh weight of frozen samples were homogenized in a pre-chilled Mixer Mill (MM 400, Retsch) with 1 ml of ice-cold extraction buffer consisting of 100 mM Bicine-NaOH CO_2-free (pH 8.1), 1 mM EDTA, 10 mM DTT, 50 mM β-mercaptoethanol, 20 mM $MgCl_2$, 1 mM benzamidine, 1 mM ε-aminocaproic acid, 1% plant protease inhibitor cocktail (P9599, Sigma-Aldrich), 2 mM phenylmethylsulfonyl fluoride, 0.5% Triton X-100, 25 mg ml^{-1} polyvinylpolypyrrolidone, and a saturating concentration of $NaHCO_3$ (10 mM, 20 mM, or 40 mM depending on the species). The homogenate was immediately centrifuged for 10 min at 20,000 *g* and 4 °C. Total soluble protein was determined in the supernatant according to the method of Bradford (1976). Part of the supernatant was then supplemented with sufficient carrier-free $NaH^{14}CO_3$ to adjust the specific radioactivity to 3.7×10^{10} Bq mol^{-1} (1 Ci mol^{-1}) and incubated for 15–20 min at 25 °C for full activation of Rubisco. Rates of Rubisco $^{14}CO_2$ fixation were measured in 8 ml septum-sealed glass vials with magnetic stirring, under a 100% N_2 atmosphere. The vials contained assay buffer, consisting of 100 mM Bicine-NaOH CO_2-free (pH 8.1), 20 mM $MgCl_2$, 1.5 mM ribulose-1,5-bisphosphate (RuBP; R0878, Sigma-Aldrich) and ~100 W-A units of carbonic anhydrase (C3934, Sigma-Aldrich), previously sparged with 100% N_2, and one of eight concentrations of $NaH^{14}CO_3$ from 0.2 to 18 mM for the assays at 25 °C and from 0.2 to 6 mM for the assays at 4 °C (except for the green algae, for which $NaH^{14}CO_3$ concentrations from 0.8 to 49 mM for the assays at 25 °C and from 0.8 to 17 mM for the assays at 4 °C were used), each with a specific radioactivity of 3.7×10^{10} Bq mol^{-1}. Assays (0.5 ml final volume) were started by the injection of 10–20 µl of activated algal extract and stopped with the addition of 200 µl 1 M formic acid after 1 min (for the assays at 25 °C) or 2 min (for the assays at 4 °C). The acidified samples were dried at 80 °C and the acid-stable ^{14}C-organic molecules were determined by scintillation counting (Beckman Coulter LS 6500). Values for K_c and maximum carboxylase activity (V_{max}^c) were extrapolated from the data fitted to the Michaelis–Menten equation as described by Sharwood *et al.* (2008) and Whitney *et al.* (2011). Concentrations of CO_2 in solution were calculated assuming an acid dissociation constant (pK_a) for carbonic acid of 6.28 at 4 °C and 6.11 at 25 °C (Galmés *et al.*, 2016), a solubility constant for CO_2 of 0.0626 mol l^{-1} atm^{-1} at 4 °C and 0.034 mol l^{-1} atm^{-1} at 25 °C, and using accurate measures of the pH (NBS scale) of each buffer solution at the respective assay temperature. Replicate measurements (n=3–5) were made using independent crude protein extracts from different individuals. A series of assays of *Triticum aestivum* L. cv. Cajeme was interspersed with those of the algal species analyzed as an external control, yielding values similar to those recently reported in the literature (Hermida-Carrera *et al.*, 2016; Table 2).

k_{cat}^c was calculated by dividing V_{max} by the concentration of Rubisco active sites, which was quantified from the same crude protein extracts

Table 1. *Location, origin, evolutionary history, depth zonation, optimum temperature for growth (T_{growth}), and upper survival temperature (UST) of the seaweed populations studied*

Species	Location of sampling	Origin	Depth of collection below sea level (m)	Evolutionary history	Depth zonation	T_{growth} (°C)	UST (°C)	References for T_{growth} and UST
Rhodophyta								
Phycodrys rubens (L.) Batters	Kongsfjord (Spitsbergen)	Natural population	15	Non-endemic	Lower sublittoral	10	n.d.	Novaczek *et al.* (1990)
Phycodrys rubens (L.) Batters	Helgoland (Germany)	Natural population	6–8	Non-endemic	Lower sublittoral	n.d.	18–20	Lüning (1984)
Ptilota gunneri Silva, Maggs & Irvine	Kongsfjord (Spitsbergen)	Natural population	10	Non-endemic	Lower sublittoral	4–10	n.d.	Gordillo *et al.* (2016)
Devaleraea ramentacea (L.) Guiry	Kongsfjord (Spitsbergen)	Natural population	2–3	Arctic Endemic	Upper sublittoral	0–10 (0)	18–20	Novaczek *et al.* (1990); Bischoff and Wiencke (1993)
Palmaria palmata (L.) Weber & Mohr	Kongsfjord (Spitsbergen)	AWI collection (2265)	–	Non-endemic	Upper sublittoral	12	n.d.	Van de Poll *et al.* (2002)
Palmaria palmata (L.) Weber & Mohr	Roscoff (France)	AWI collection	–	Non-endemic	Lower eulittoral/upper sublittoral	12	n.d.	Van de Poll *et al.* (2002)
Palmaria decipiens (Reinsch) Ricker	King George Island (Antarctica)	AWI collection (2113)	–	Antarctic Endemic	Mid eulittoral/upper sublittoral	5	15–16	Wiencke and tom Dieck (1989)
Ochrophyta (Phaeophyceae)								
Alaria esculenta (L.) Greville	Kongsfjord (Spitsbergen)	Natural population	10	Non-endemic	Mid sublittoral	4–10	n.d.	Gordillo *et al.* (2016)
Desmarestia aculeata (L.) Lamouroux	Kongsfjord (Spitsbergen)	Natural population	5	Non-endemic	Mid sublittoral	5	20	Bischoff and Wiencke (1993)
Laminaria solidungula J.Agardh	Kongsfjord (Spitsbergen)	Natural population	4–6	Arctic Endemic	Mid sublittoral	5–10	16	tom Dieck (1992)
Laminaria digitata (Huds.) Lamouroux	Kongsfjord (Spitsbergen)	Natural population	5	Non-endemic	Mid sublittoral	10	n.d.	Bolton and Lüning (1982)
Saccharina latissima (L.) Lane, Mayes, Druehl, Saunders	Kongsfjord (Spitsbergen)	AWI collection (3123,3124)	–	Non-endemic	Mid sublittoral	10	n.d.	Olischläger *et al.* (2017)
Saccharina latissima (L.) Lane, Mayes, Druehl, Saunders	Helgoland (Germany)	AWI collection (3094,3096)	–	Non-endemic	Mid sublittoral	10–20 (15)	18–20	Fortes and Lüning (1980)
Himantothallus grandifolius (A. & E.S.Gepp) Zinova	King George Island (Antarctica)	AWI collection (3006,3010)	–	Antarctic Endemic	Mid to lower sublittoral	0–5	11–13	Wiencke and tom Dieck (1989)
Chlorophyta								
Acrosiphonia arcta (Dillwyn) Gain	Disko Island (Greenland)	AWI collection (1120)	–	Non-endemic	Upper sublittoral	0–10	22	Bischoff and Wiencke (1995)
Acrosiphonia arcta (Dillwyn) Gain	Helgoland (Germany)	AWI collection (1083)	–	Non-endemic	Lower eulittoral	5–15	22	Bischoff and Wiencke (1995)
Acrosiphonia arcta (Dillwyn) Gain	King George Island (Antarctica)	AWI collection (1160)	–	Non-endemic	Lower eulittoral	5	22	Bischoff and Wiencke (1995)

n.d., Not determined.

Table 2. *Rubisco carboxylation kinetics of the analyzed polar populations measured at 25 °C and 4 °C, the ratio between 25 °C and 4 °C measurements for each kinetic parameter, and Rubisco content at the growth conditions*

Species	K_c (μM)			k_{cat}^c (s^{-1})			k_{cat}^c/K_c (s^{-1} mM^{-1})			[Rubisco]/[TSP] (%)
	25 °C	4 °C	25 °C/4 °C	25 °C	4 °C	25 °C/4 °C	25 °C	4 °C	25 °C/4 °C	
Rhodophyta										
Phycodrys rubens	18.9±0.8	4.8±0.7	3.94±0.40	1.76±0.03	0.14±0.01	12.2±0.9	93.5±3.8	30.1±2.0	3.11±0.10	8.0±0.7
Ptilota gunneri	14.4±1.1	5.1±0.6	2.83±0.12	1.60±0.23	0.17±0.03	9.3±0.5	110.7±7.2	33.8±2.4	3.27±0.05	6.6±0.9
Devaleraea ramentacea	17.5±1.0	5.6±0.8	3.13±0.26	2.59±0.16	0.34±0.04	7.6±0.6	148.1±8.3	60.9±0.9	2.43±0.14	7.4±1.7
Palmaria palmata	15.9±0.6	4.9±0.2	3.24±0.01	2.08±0.05	0.27±0.01	7.8±0.2	131.3±8.1	54.6±2.1	2.40±0.07	9.9±0.6
Palmaria decipiens	17.4±1.2	5.0±0.2	3.50±0.12	2.43±0.16	0.31±0.01	7.8±0.2	139.7±3.3	62.9±0.3	2.22±0.05	7.8±0.1
Ochrophyta (Phaeophyceae)										
Alaria esculenta	23.6±1.0	4.1±0.5	5.85±1.01	2.13±0.14	0.23±0.02	9.5±1.3	90.3±4.3	55.5±1.9	1.63±0.06	17.4±1.8
Desmarestia aculeata	13.3±0.6	2.1±0.3	6.44±0.89	1.37±0.12	0.12±0.02	11.3 ±1.3	103.3±12	61.0±22	1.79±0.41	17.7±4.7
Laminaria solidungula	18.5±1.3	3.9±0.8	4.96±1.23	1.60±0.12	0.17±0.02	9.2±0.7	86.6±6.2	47.1±14	1.92±0.41	30.1±1.4
Laminaria digitata	17.0±1.0	4.0±0.3	4.25±0.40	1.42±0.28	0.10±0.02	16.4±2.9	84.3±20	26.1±2.8	3.84±0.36	24.7±7.5
Saccharina latissima	19.4±1.2	3.8±0.4	4.99±0.29	1.79±0.18	0.16±0.03	10.8±0.6	92.5±7.5	43.3±8.4	2.17±0.23	37.3±6.1
Himantothallus grandifolius	18.1±1.1	4.4±0.8	4.14±0.49	2.08±0.02	0.23±0.01	9.2±0.6	115±7.4	51.7±6.5	2.23±0.16	n.d.
Chlorophyta										
Acrosiphonia arcta (Arctic)	52.8±1.6	17.7±2.6	3.01±0.33	5.08±0.15	0.82±0.03	6.2±0.1	96.2±2.7	46.7±5.7	2.07±0.22	7.6±0.1
Control										
Triticum aestivum	9.6±0.4	3.1±0.1	3.06±0.14	2.20±0.23	0.20±0.01	11.2±0.6	230.1±28	62.8±4.1	3.66±0.28	42.3±2.5

k_{cat}^c, Rubisco carboxylase turnover rate; K_c, Michaelis–Menten affinity constant for CO_2; k_{cat}^c/K_c, carboxylation efficiency; [Rubisco]/[TSP], percentage of Rubisco in the total soluble protein. Data are means ±SD (n=3–5 independent thalli). n.d., Not determined.

by 2′-carboxyarabinitol-1,5-bisphosphate (^{14}C-CABP) binding (Ruuska *et al.*, 1998), assuming eight binding sites per Rubisco (Blayney *et al.*, 2011). Our preliminary assays revealed that analyzed red and brown seaweed Rubiscos need an increased CABP concentration (up to 1.2 mM) for saturating Rubisco active sites than that previously used for form IB Rubiscos (29–80 μM; Ruuska *et al.*, 1998; Kubien *et al.*, 2011). These results agree well with those from Pearce (2006) showing a 100-fold higher semi-saturation constant for CABP inhibition and 2-fold slower binding of form ID than form IB Rubisco active sites. A 15 μl aliquot of activated extract was incubated with ^{14}C-CABP for 30 min at room temperature before chromatographic separation of Rubisco-bound and free ^{14}C-CABP. Previous incubation of the mixture for up to 24 h at 4 °C followed by 30 min at room temperature before chromatographic separation did not significantly increase ^{14}C-CABP binding. Immunoblotting of the crude protein extracts using a Rubisco large subunit antibody and purified spinach Rubisco standard (AS03 037 and AS01 017S, Agrisera) gave similar values of Rubisco concentration to those obtained by ^{14}C-CABP binding (data not shown).

Carboxylation assay controls at saturating $NaH^{14}CO_3$ concentrations either without RuBP addition or with activated algal extract pre-incubated for 30 min with non-radioactive CABP (up to 1.2 mM) were carried out in order to confirm that the observed acid-stable ^{14}C was only the result of Rubisco catalytic activity. Both controls gave values lower than 5% of the maximum activity in all analyzed species. Saturating concentrations of RuBP, ^{14}C-CABP, and $H^{14}CO_3^-$, as well as the optimum incubation time and temperature for full Rubisco activation, were determined in preliminary assays. RuBP of ≥90% purity (R0878, Sigma-Aldrich) and of ≥99% purity (83895, Sigma-Aldrich) were also compared, obtaining no significant differences in Rubisco kinetics at saturating conditions.

Data analysis

Significance of differences between populations of the same species (n=3–5) were tested using one-way analysis of variance, after normality (Shapiro–Wilk test) and homogeneity of variances were confirmed. Post hoc comparisons were performed using Fisher's least significant difference test. Pearson correlation coefficients were obtained for the significance of the association between different variables. The confidence interval for all these tests was set at 95% (P≤0.05). All statistical analyses were performed using SigmaPlot 12.0 statistical software (Systat Software Inc.).

Results

Variability in Rubisco kinetics and its thermal response among polar seaweeds

At 25 °C, when considering only form ID Rubiscos (i.e. rhodophytes and ochrophytes), K_c and k_{cat}^c varied ~2-fold among species (Table 2). The lowest values corresponded to *Desmarestia aculeata* (K_c=13.3 μM, k_{cat}^c=1.37 s^{-1}) and the highest values were found in *Alaria esculenta* for K_c (23.6 μM) and in *Devaleraea ramentacea* for k_{cat}^c (2.59 s^{-1}). Rubisco from *A. arcta*, the only chlorophyte included in the study, had the highest values for K_c and k_{cat}^c, which were two to four times higher than those found in the other species.

The highest values of k_{cat}^c/K_c were found for the polar endemic species *Palmaria decipiens* (140 s^{-1} mM^{-1}) and *D. ramentacea* (148 s^{-1} mM^{-1}), while the lowest value was obtained for *Laminaria digitata* (84.3 s^{-1} mM^{-1}; Table 2). The Antarctic endemic species *Himantothallus grandifolius* presented the highest value among the ochrophytes (115 s^{-1} mM^{-1}). The chlorophyte *A. arcta* had a k_{cat}^c/K_c in the range of the other species.

The percentage of Rubisco in the total soluble protein ([Rubisco]/[TSP]) was highly variable among the species, ranging from 6.6% in *Ptilota gunneri* to 37.3% in *S. latissima* (Table 2).

The range of variation for K_c and k_{cat}^c was smaller at 4 °C compared with 25 °C (Table 2). Among form ID Rubiscos, at 4 °C, K_c and k_{cat}^c ranged from 2.1 μM (*D. aculeata*) and 0.1 s^{-1} (*L. digitata*) to 5.6 μM and 0.34 s^{-1} (both for *D. ramentacea*), respectively. The chlorophyte *A. arcta* again showed the highest values for K_c and k_{cat}^c at 4 °C, with values being three to eight times higher than those in the remaining species. At 4 °C, the species showing maximum and minimum values of k_{cat}^c/K_c were the same as those identified at 25 °C, with the exception of *D. aculeata*, which presented one of the highest values (61 s^{-1} mM^{-1}).

Regarding thermal dependencies of the different kinetics parameters, the ratio $(K_c)^{25\,°C}/(K_c)^{4\,°C}$ varied between 2.83 for *Ptilota gunneri* and 6.44 for *D. aculeata*, while $(k_{cat}^c)^{25\,°C}/(k_{cat}^c)^{4\,°C}$ ranged from 6.2 in *A. arcta* to 16.4 in *L. digitata* (Table 2). The lowest value of $(k_{cat}^c)^{25\,°C}/(k_{cat}^c)^{4\,°C}$ within the Rhodophyta was obtained for the Arctic endemic species *D. ramentacea* (7.6), and within the Ochrophyta, for the two polar endemic species *Laminaria solidungula* and *H. grandifolius* (9.2), whereas $(k_{cat}^c/K_c)^{25\,°C}/(k_{cat}^c/K_c)^{4\,°C}$ varied from 1.63 in *A. esculenta* to 3.84 in *L. digitata*.

Intraspecific differences in Rubisco kinetics and its thermal response between polar and cold-temperate populations

For *Phycodrys rubens*, the only statistically significant difference between the Arctic and cold-temperate populations was found in K_c and k_{cat}^c/K_c at 25 °C, consisting of a lower affinity for CO_2 and a lower carboxylation efficiency in the polar population compared with the Atlantic population (Table 3). These differences at 25 °C were not found at 4 °C, and, furthermore, [Rubisco]/[TSP], k_{cat}^c, and the ratio 25 °C/4 °C for the different kinetic parameters were not significantly different between the two populations.

For *Palmaria palmata*, the Arctic population displayed ~15% higher k_{cat}^c and k_{cat}^c/K_c at 4 °C compared with the Atlantic population (Table 3). Non-significant differences were observed between the two populations in K_c, [Rubisco]/[TSP], and the ratio 25 °C/4 °C for the different kinetic parameters.

The Arctic population of *S. latissima* had a higher k_{cat}^c at 4 °C compared with the cold-temperate population, together with a higher k_{cat}^c/K_c at both assayed temperatures (65% higher at 4 °C; see Table 3). As a consequence, the ratios $(k_{cat}^c)^{25\,°C}/(k_{cat}^c)^{4\,°C}$ and $(k_{cat}^c/K_c)^{25\,°C}/(k_{cat}^c/K_c)^{4\,°C}$ were lower in polar *S. latissima* relative to the Atlantic population, while [Rubisco]/[TSP] was similar in the two populations.

The Antarctic population of *A. arcta* showed the lowest K_c at 25 °C, followed by the Arctic population, in comparison to the cold-temperate population; this difference was reflected in a higher k_{cat}^c/K_c for the Antarctic population (Table 3). At 4 °C, non-significant differences in k_{cat}^c/K_c were found among the three populations, despite the higher k_{cat}^c for the Antarctic population. Most noticeably, [Rubisco]/[TSP] was ~150%

Table 3. *Rubisco carboxylation kinetics of the polar and cold-temperate populations of the same species measured at 25 °C and 4ºC, the ratio between 25 °C and 4 °C measurements for each kinetic parameter, and Rubisco content at the growth conditions (data corresponding to the polar populations are also shown in Table 2)*

Species	K_c (μM)			k_{cat}^c (s^{-1})			k_{cat}^c/K_c (s^{-1} mM^{-1})			[Rubisco]/[TSP] (%)
	25 °C	4 °C	25 °C/4 °C	25 °C	4 °C	25 °C/4 °C	25 °C	4 °C	25 °C/4 °C	
Rhodophyta										
Phycodrys rubens (Arctic)	18.9±0.8 ^{b}	4.8±0.7 ^{a}	3.94±0.40 ^{a}	1.76±0.03 ^{a}	0.14±0.01 ^{a}	12.2±0.9 ^{a}	93.5±3.8 ^{a}	30.1±2.0 ^{a}	3.11±0.10 ^{a}	8.0±0.7 ^{a}
Phycodrys rubens (Helgoland)	15.7±0.7 ^{a}	5.3±1.9 ^{a}	3.24±1.14 ^{a}	1.92±0.19 ^{a}	0.16±0.03 ^{a}	12.1±1.3 ^{a}	122±10.6 ^{b}	31.9±6.8 ^{a}	3.95±0.90 ^{a}	8.5±0.3 ^{a}
Palmaria palmata (Arctic)	15.9±0.6 ^{a}	4.9±0.2 ^{a}	3.24±0.01 ^{a}	2.08±0.05 ^{b}	0.27±0.01 ^{b}	7.8±0.2 ^{a}	131.3±8.1 ^{a}	54.6±2.1 ^{b}	2.40±0.07 ^{a}	9.9±0.6 ^{a}
Palmaria palmata (Roscoff)	14.9±0.8 ^{a}	4.6±0.1 ^{a}	3.22±0.22 ^{a}	1.85±0.04 ^{a}	0.23±0.01 ^{a}	8.2±0.3 ^{a}	124.8±9.4 ^{a}	49.1±2.6 ^{a}	2.54±0.09 ^{a}	9.4±0.2 ^{a}
Ochrophyta (Phaeophyceae)										
Saccharina latissima (Arctic)	19.4±1.2 ^{a}	3.8±0.4 ^{a}	4.99±0.29 ^{a}	1.79±0.18 ^{a}	0.16±0.03 ^{b}	10.8±0.6 ^{a}	92.5±7.5 ^{b}	43.3±8.4 ^{b}	2.17±0.23 ^{a}	37.3±6.1 ^{a}
Saccharina latissima (Helgoland)	19.6±0.5 ^{a}	4.2±0.6 ^{a}	4.75±0.61 ^{a}	1.34±0.44 ^{a}	0.11±0.04 ^{a}	12.6±0.7 ^{b}	68.1±21.5 ^{a}	26.3±10 ^{a}	2.69±0.38 ^{b}	36.6±6.4 ^{a}
Chlorophyta										
Acrosiphonia arcta (Arctic)	52.8±1.6 ^{b}	17.7±2.6 ^{a}	3.01±0.33 ^{a}	5.08±0.15 ^{a}	0.82±0.03 ^{a}	6.19±0.07 ^{c}	96.2±2.7 ^{b}	46.7±5.7 ^{a}	2.07±0.22 ^{b}	7.6±0.1 ^{b}
Acrosiphonia arcta (Helgoland)	57.4±1.6 ^{c}	16.4±0.6 ^{a}	3.49±0.16 ^{a}	4.89±0.06 ^{a}	0.82±0.02 ^{a}	5.94±0.11 ^{b}	85.3±2.9 ^{a}	50.1±0.9 ^{a}	1.70±0.09 ^{a}	2.9±0.4 ^{a}
Acrosiphonia arcta (Antarctic)	48.2±0.9 ^{a}	15.6±1.5 ^{a}	3.10±0.25 ^{a}	4.99±0.02 ^{a}	0.86±0.01 ^{b}	5.78±0.06 ^{a}	103.5±2.0 ^{c}	55.0±6.0 ^{a}	1.87±0.16 ^{ab}	6.9±1.4 ^{b}

k_{cat}^c, Rubisco carboxylase turnover rate; K_c, Michaelis–Menten affinity constant for CO_2; k_{cat}^c/K_c, carboxylation efficiency; [Rubisco]/[TSP], percentage of Rubisco in the total soluble protein. Different letters indicate statistically significant differences ($P<0.05$) between populations of the same species. Data are means ±SD ($n=3–5$ independent thalli).

higher in the two polar populations compared with the cold-temperate population.

Carbon utilization of polar versus cold-temperate populations

Among all the species, only two of them (the lower sublittoral rhodophytes *Phycodrys rubens* and *Ptilota gunneri*) displayed values of $\delta^{13}C_{alga}$ <–30‰ and pH compensation point ≤9 (Table 4). A positive correlation was found between $\delta^{13}C_{alga}$ and pH compensation point among all seaweed species studied (R=0.921, P<0.001, Fig. 1) and also when considering species with form ID Rubisco exclusively (R=0.891, P<0.001). As shown in Fig. 1, there was a striking separation into two groups, one for the species growing in the mid to lower sublittoral, with $\delta^{13}C_{alga}$ <–25‰ and pH compensation point <10, and the other for the species growing in the upper sublittoral to lower eulittoral, with $\delta^{13}C_{alga}$ >–25‰ and pH compensation point >10.

All polar populations showed a significantly higher pH compensation point and/or less negative $\delta^{13}C_{alga}$ values than their cold-temperate counterparts (Table 4). The Atlantic population of *Phycodrys rubens* had a slightly more negative $\delta^{13}C_{alga}$ value than its polar counterpart, although both values were lower than –30‰. The pH compensation point found in the *Palmaria palmata* population from Roscoff was lower than that from the polar population of the same species, whereas the $\delta^{13}C_{alga}$ values were similar. For *S. latissima,* the $\delta^{13}C_{alga}$ value was lower in the Helgoland population relative to the polar population. The Atlantic *A. arcta* showed lower $\delta^{13}C_{alga}$ and pH compensation point values than the Arctic and Antarctic populations of this species.

Table 4. *Stable carbon isotope discrimination values ($\delta^{13}C_{alga}$) and pH compensation points of the analyzed seaweed populations*

Species	$\delta^{13}C_{alga}$ (‰)	pH compensation point
Rhodophyta		
Phycodrys rubens (Arctic)	–36.5±0.4 [a]	9.04±0.03
Phycodrys rubens (Helgoland)	–37.4±0.5 [b]	n.d.
Ptilota gunneri	–36.4±0.8	8.93±0.02
Devaleraea ramentacea	–24.2±0.4	10.59±0.04
Palmaria palmata (Arctic)	–18.6±2.4 [a]	10.78±0.06 [b]
Palmaria palmata (Roscoff)	–18.7±2.7 [a]	10.39±0.04 [a]
Palmaria decipiens	–19±1.3	10.78±0.09
Ochrophyta (Phaeophyceae)		
Alaria esculenta	–28.4±1.2	9.33±0.05
Desmarestia aculeata	–26.7±2.9	9.34±0.04
Laminaria solidungula	–29.3±0.8	9.44±0.05
Laminaria digitata	–25.6±1.2	9.61±0.05
Saccharina latissima (Arctic)	–21.8±0.8 [a]	n.d.
Saccharina latissima (Helgoland)	–23.7±1.4 [b]	n.d.
Himantothallus grandifolius	–25.2±0.5	9.53±0.06
Chlorophyta		
Acrosiphonia arcta (Arctic)	–15.1±0.6 [a]	10.91±0.01 [b]
Acrosiphonia arcta (Helgoland)	–20±0.3 [c]	10.37±0.03 [a]
Acrosiphonia arcta (Antarctic)	–16.8±1 [b]	10.83±0.01 [b]

Different letters indicate statistically significant differences (P<0.05) between populations of the same species. Data are means ±SD (n=4–5 independent thalli). n.d., Not determined.

Trade-off among Rubisco carboxylation kinetics and their relationship with carbon utilization

When analyzing the data from all species assayed at both 4 °C and 25 °C, k_{cat}^{c} and K_c correlated positively (R=0.958, P<0.001). The same correlation was also found when considering the species with form ID Rubisco exclusively (R=0.935, P<0.001). At each assay temperature, the correlation between k_{cat}^{c} and K_c was significant when all species were analyzed together (R=0.951, P<0.001 at 25 °C and R=0.971, P<0.001 at 4 °C; Fig. 2). However, the analysis of form ID Rubiscos alone revealed a significant correlation only between k_{cat}^{c} and K_c at 4 °C (R=0.555, P<0.05), and not at 25 °C (R=0.211, P=0.47, Fig. 2).

Generally, a larger number of significant correlations was obtained between Rubisco kinetics and either $\delta^{13}C_{alga}$ values, pH compensation points, or the ratio [Rubisco]/[TSP] when all species were analyzed together than when the three populations of the chlorophyte *A. arcta* were excluded from the analysis (Table 5). [Rubisco]/[TSP] correlated negatively with k_{cat}^{c}/K_c at 25 °C. The significant negative correlation between [Rubisco]/[TSP] and k_{cat}^{c} at both 4 °C and 25 °C was lost when only form ID Rubiscos were analyzed. A positive relationship was found between k_{cat}^{c} measured at both temperatures and the pH compensation point. The ratio k_{cat}^{c}/K_c at 25 °C correlated positively with the pH compensation point only for form ID Rubiscos. Conversely, all significant correlations between $\delta^{13}C_{alga}$ and Rubisco kinetics were lost when only form ID Rubiscos were analyzed (Table 5).

Discussion

Variability in Rubisco carboxylation kinetics

The K_c values obtained in the present study at 25 °C (Tables 2 and 3) fell within the wide range reported for the few seaweed species analyzed in previous studies, between 9.3 μM in *Griffithsia monilis* (Whitney *et al.*, 2001) and 70 μM in *Ulva* sp. (Yeoh *et al.*, 1981). Fig. 3 represents a compilation of our results and previously published carboxylation kinetics measured at 25 °C for other phylogenetic groups possessing form I Rubisco (see Supplementary Table S1 at *JXB* online), showing that brown seaweeds (Phaeophyceae) display lower K_c and k_{cat}^{c} values at 25 °C than diatoms (Bacillariophyceae), and lower k_{cat}^{c} but similar K_c to haptophytes (which also possess form ID Rubisco). On the other hand, red seaweeds (Florideophyceae) present higher K_c and k_{cat}^{c} values and lower k_{cat}^{c}/K_c than red algae belonging to the family

Cyanidiophyceae. These differences reveal a large variation within form ID Rubisco kinetics.

Rubisco K_c values from brown and red seaweeds, along with those from haptophytes, were similar to those of C_4 plants and higher than those of C_3 plants, whereas chlorophytes and diatoms displayed the highest K_c values within the eukaryotes (Fig. 3C). These differences in K_c might be related to the presence and strength of CCMs. However, the same differences were not observed in k_{cat}^c values (Fig. 3B), leading to lower carboxylation efficiencies (k_{cat}^c/K_c) in all seaweeds analyzed in the present study relative to C_3 vascular plants; this seems to be a general pattern within marine algae (Fig. 3A). Moreover, Ochrophyta and Chlorophyta also showed significantly lower k_{cat}^c/K_c than C_4 vascular plants.

The absence of a significant correlation between K_c and k_{cat}^c at 25 °C when only red and brown seaweed Rubiscos were analyzed is in agreement with the results of Young *et al.* (2016) and Heureux *et al.* (2017) for other form ID Rubiscos. These results suggest that the canonical trade-off typically observed between K_c and k_{cat}^c for plants, which was thought to be due to a fundamental mechanistic constraint of their interrelated rate constants (Tcherkez *et al.*, 2006), might not be universal for all Rubiscos. Differences in the relationship between k_{cat}^c and K_c may arise from differences in the intrinsic equilibrium of the RuBP enolization reaction (Tcherkez, 2013).

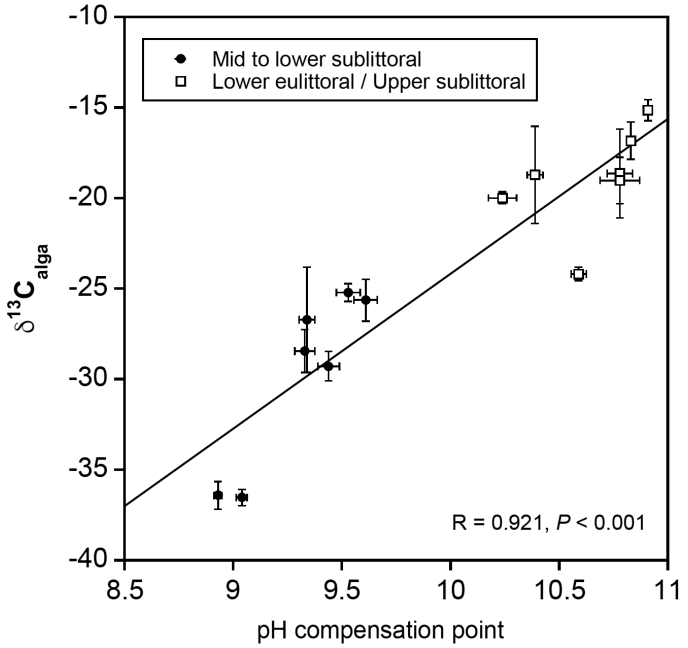

Fig. 1. Relationship between the pH compensation point and carbon isotope discrimination ($\delta^{13}C_{alga}$) from all analyzed seaweed populations. Filled circles represent populations distributed in the mid to lower sublittoral and open squares represent populations distributed in the lower sublittoral and/or upper sublittoral. Data are presented as mean ±SD (n=4–5).

Co-evolution of Rubisco and CCMs in seaweeds

It has previously been demonstrated that Rubisco kinetics of organisms from other phylogenetic groups have a strong correlation with CCMs, showing higher values of k_{cat}^c and K_c for Rubiscos adapted to higher $[CO_2]$:$[O_2]$ ratios (Tcherkez *et al.*, 2006; Savir *et al.*, 2010; Whitney *et al.*, 2011). The positive correlation observed in the present study between Rubisco kinetic parameters and the CCM proxies, $\delta^{13}C_{alga}$ and pH compensation point, for all species analyzed together (Table 5) is in agreement with these previous reports. By contrast, when only form ID Rubiscos were analyzed, K_c was correlated with neither $\delta^{13}C_{alga}$ nor the pH compensation point, although k_{cat}^c was positively correlated with the pH compensation point at both assay temperatures studied. These results suggest a positive selection in form ID Rubisco k_{cat}^c from macroalgae possessing CCMs without a significant concomitant increase in K_c, diverging from the canonical trade-off between K_c and k_{cat}^c.

It is important to consider that, unlike in C_4 plants, the expression of CCMs in algae is facultative, and is regulated by a large number of environmental factors (Giordano *et al.*, 2005).

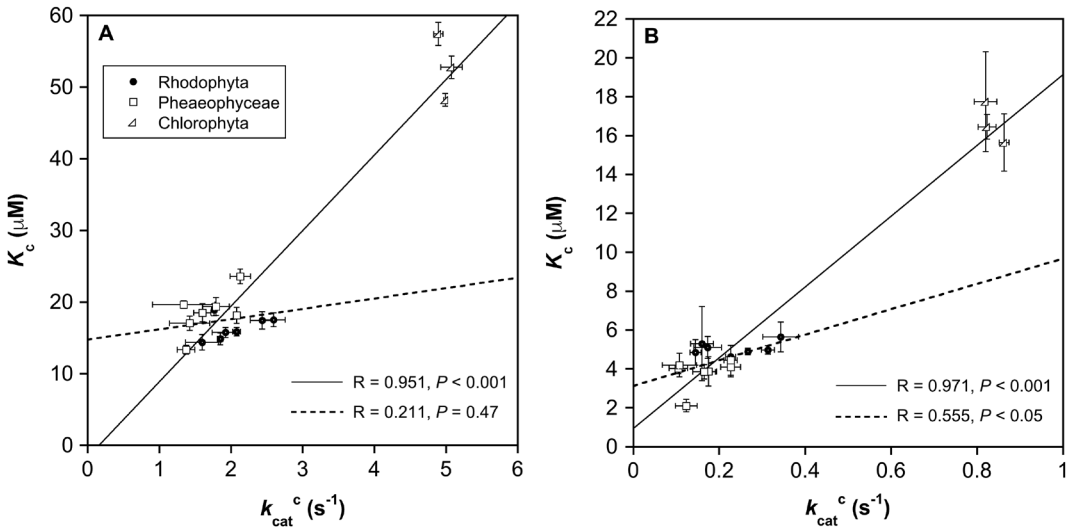

Fig. 2. Trade-off between the maximum carboxylation rate (k_{cat}^c) and the Michaelis–Menten affinity constant for CO_2 (K_c) for the analyzed seaweed Rubiscos at (A) 25 °C and (B) 4 ° C. The solid line represents the correlation of all populations together (including chlorophytes); the dashed line represents the correlation of form ID Rubiscos alone. Data are presented as mean ±SD (n=3–5).

Table 5. *Pearson's correlation coefficients between the Rubisco kinetic parameters at 25 °C and 4 °C and either the percentage of Rubisco in the total soluble protein, ^{13}C isotope discrimination, or pH compensation point, considering (A) all 17 seaweed populations together, and (B) the 14 red and brown seaweed populations (all possessing form ID Rubiscos) alone*

(A) Data from all populations analyzed together						
	25 °C			**4 °C**		
	K_c	k_{cat}^c	k_{cat}^c/K_c	K_c	k_{cat}^c	k_{cat}^c/K_c
$\delta^{13}C_{alga}$	0.505*	0.57*	0.1	0.502*	0.601*	0.514*
pH compensation point	0.455	0.637*	0.488	0.554*	0.65*	0.519
[Rubisco]/[TSP]	–0.34	–0.519*	–0.575*	–0.476	–0.513*	–0.339
(B) Data from red and brown algal species (Form ID Rubiscos)						
	25 °C			**4 °C**		
	K_c	k_{cat}^c	k_{cat}^c/K_c	K_c	k_{cat}^c	k_{cat}^c/K_c
$\delta^{13}C_{alga}$	0.01	0.27	0.26	0.13	0.44	0.518
pH compensation point	–0.15	0.669*	0.806**	0.41	0.777**	0.573
[Rubisco]/[TSP]	0.42	–0.545	–0.768**	–0.549	–0.536	–0.29

k_{cat}^c/K_c, carboxylation efficiency; k_{cat}^c, carboxylase turnover rate; K_c, Michaelis–Menten affinity constant for CO_2; [Rubisco]/[TSP], percentage of Rubisco in the total soluble protein; $\delta^{13}C_{alga}$, ^{13}C isotope discrimination. *P<0.05, **P<0.01, ***P<0.001.

Thus, pH drift experiments must indicate the presence of a potential CCM capacity, since long-term exposure under constant and saturating irradiance to decreasing CO_2 concentrations as the pH increases may lead to the expression of CCM components (Raven *et al.*, 2005). In contrast, $\delta^{13}C_{alga}$ values might reflect CCM operation during the growth of the thalli, which could be down-regulated due to energetic constraints (Hepburn *et al.*, 2011). Despite the different timescales of both measurements, a positive correlation between $\delta^{13}C_{alga}$ and pH compensation point was found, along with a striking separation between intertidal and subtidal species for these measurements (see Fig. 1); similar observations were previously reported in a global meta-analysis including 141 marine macrophyte species (Stepien, 2015).

Since $\delta^{13}C_{alga}$ values could be influenced not only by the isotopic composition of the C_i source but also by CO_2 leakage (Sharkey and Berry, 1985), these data should be treated with caution when used as a proxy for CCM operation. High CO_2 leakage prevents the accumulation of $\delta^{13}C_{alga}$ within the intracellular carbon pool, thereby decreasing $\delta^{13}C_{alga}$, which must approach the Rubisco isotope fractionation. Moreover, Rubisco isotope fractionation of the analyzed red and brown seaweeds, as previously shown for other ID Rubiscos (Boller *et al.*, 2015), might be different from that of spinach Rubisco (–30‰; Roeske and O'Leary, 1984), even though this value has been widely used as a cutoff for excluding HCO_3^- use in marine seaweeds (Maberly *et al.*, 1992; Raven *et al.*, 2002*a*). pH drift experiments could also be affected by CO_2 leakage and proton extrusion, leading to a lower pH compensation point than the one corresponding to the species' capacity for HCO_3^- use. However, these interferences might be negligible in our study because total alkalinity was not significantly altered after pH drift experiments (data not shown). Despite the possible effect of CO_2 leakage, most of the analyzed species showed pH compensation points significantly higher than 9, indicating that these species must possess the ability to use HCO_3^- for photosynthesis.

Only the lower sublittoral rhodophytes *Phycodrys rubens* and *Ptilota gunneri* showed a pH compensation point ≤9; these species were also the only ones with a $\delta^{13}C_{alga}$ value more negative than –30‰. Therefore, assuming the limitations explained above, these findings might suggest that photosynthesis in these species relies only on diffusive CO_2 entry. Our results are in agreement with previous studies suggesting the presence or absence of CCMs in the same species as were analyzed in the present study (Surif and Raven, 1989; Johnston *et al.*, 1991; Maberly *et al.*, 1992; Beardall and Roberts, 1999; Sherlock and Raven, 2001; Raven *et al.*, 2002*a*, 2005; Klenell *et al.*, 2004; Gordillo *et al.*, 2006; Iñiguez *et al.*, 2016*b*; Olischläger *et al.*, 2017).

All polar populations had higher or similar pH compensation point and $\delta^{13}C_{alga}$ values than their cold-temperate counterparts (Table 4), even though the dissolved CO_2 concentration of cold air-equilibrated seawater is significantly higher than at warmer temperatures (Skirrow, 1975). This fact, together with the observed strong decrease in K_c and k_{cat}^c at 4 °C, would lead to closer CO_2 saturation conditions of the analyzed form ID Rubiscos in polar air-equilibrated seawater, although Rubisco oxygenation kinetics must be analyzed in these species to further corroborate this assumption. Therefore, the maintenance or even increase of active HCO_3^- use at low temperatures might be related to the fact that equilibrium conditions are not frequently met in cold oceans owing to the thermohaline circulation, biological activity, and slow equilibration of CO_2 between the surface of the oceans and the atmosphere relative to that between CO_2 and the other DIC species (Raven and Falkowski, 1999). The solubility of O_2 also increases at low temperatures (Skirrow, 1975), and there is a considerable reduction in the uncatalyzed rate of CO_2 supply from bicarbonate (Egleston *et al.*, 2010) and the diffusion rate of CO_2 (Boudreau, 1997) in cold waters. Furthermore, the exposure to continuous light during the summer months at polar latitudes in combination with low temperatures results in the activation of photoprotection mechanisms for dissipation

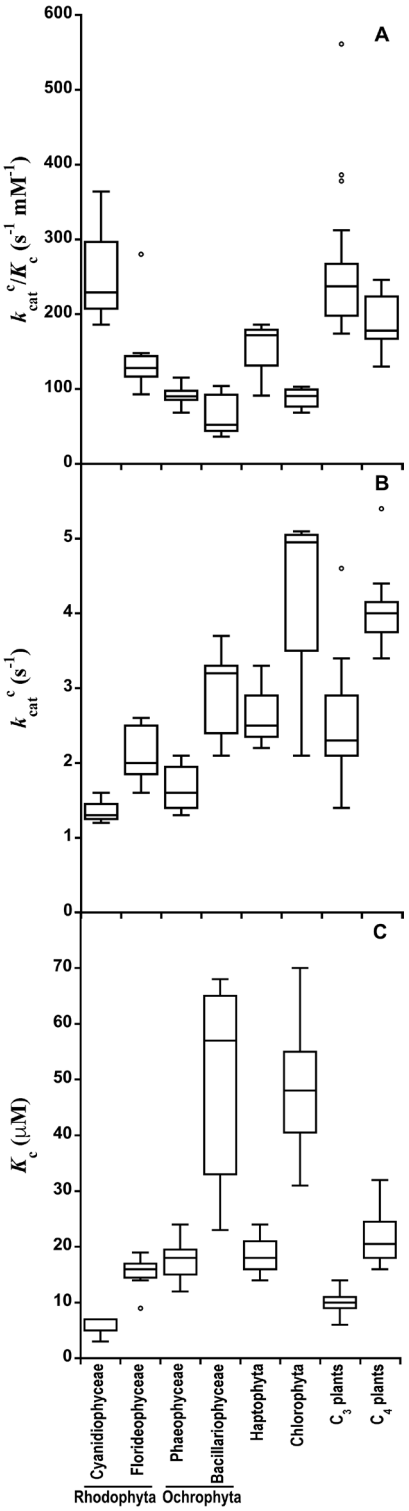

Fig. 3. Box plots depicting Rubisco carboxylation kinetics parameters at 25 °C for different taxonomic groups, including the species analyzed in this study (see Tables 2 and 4) and previous published values for others species (see Supplementary Table S1). (A) Carboxylation efficiency (k_{cat}^c/K_c); (B) carboxylase turnover rate (k_{cat}^c); (C) Michaelis–Menten affinity constant for CO_2 (K_c). For each plot, the horizontal line represents the median, the box and whiskers represent the 25th to 75th percentile and the minimum to maximum distributions of the data, respectively, and any value outside this range is displayed as an individual point.

of excess energy; one example is the relevant level of cyclic electron flow reported for Antarctic diatoms (Goldman *et al.*, 2015), so the energetically costly CCMs might be part of these photoprotection mechanisms at low temperatures (Gordillo *et al.*, 2016). It should be taken into account that the ability to use HCO_3^- for photosynthesis does not necessarily mean that C_c in steady-state photosynthesis is higher than $[CO_2]$ in the external medium. C_i uptake can operate at a lower rate than that of Rubisco carboxylation, yet still improve CO_2 fixation by lessening the degree to which the $[CO_2]$ limits Rubisco carboxylation (Koch *et al.*, 2013).

The negative correlation between [Rubisco]/[TSP] and k_{cat}^c that was obtained for all the species analyzed together (Table 5) agrees well with previous studies indicating that faster carboxylation rates of Rubisco enable these seaweeds to invest less in Rubisco relative to the total soluble protein fraction (Seemann *et al.*, 1984; Ghannoum *et al.*, 2005; Galmés *et al.*, 2014). The same trend was observed when only form ID Rubiscos were considered, although it was not statistically significant (P=0.054 for 25 °C, P=0.059 for 4 °C). Nevertheless, [Rubisco]/[TSP] must be higher in actively growing thalli than in old specimens, whereas Rubisco kinetics are constant for a particular organism, which might alter the previous correlation. In the present study, the growth rate of field samples was unknown, although young thalli were selected for the analyses when possible.

The absence of correlation between the two CCM proxies, $\delta^{13}C_{alga}$ and pH compensation point, and [Rubisco]/[TSP] (R=–0.037, P=0.893 and R=–0.444, P=0.128, respectively) contrasts with previous results found in comparisons of C_3 and C_4 plants that indicated a lower [Rubisco]/[TSP] in C_4 plants owing to the contribution of proteins involved in CCMs to total soluble protein and less investment in Rubisco (Ghannoum *et al.*, 2005). However, in algae, many CCM proteins are insoluble membrane transporters, and soluble carbonic anhydrases might be also present in organisms without CCMs (Beer *et al.*, 2014). Remarkably, brown seaweeds were found to have 3-fold to 4-fold higher [Rubisco]/[TSP] than red and green macroalgae (Tables 2 and 3), which could be related to the high productivity of Laminariales and Desmarestiales underwater forests in cold-temperate to polar waters (Wiencke *et al.*, 2007). Alternatively, differences in [Rubisco]/[TSP] between groups could be partly related to a lower efficiency in the extraction of proteins other than Rubisco in the studied brown seaweeds, due to the presence of high contents of secondary metabolites and polysaccharides in these species that might interfere with protein solubilization. Very efficient total protein extraction protocols have been developed for Laminariales (Olischläger *et al.*, 2014), but these protocols unavoidably involve protein denaturation.

Intraspecific adaptation of seaweed Rubiscos to low temperatures

The Arctic populations of *Palmaria palmata* and *S. latissima* presented significantly higher k_{cat}^c/K_c at 4 °C than their temperate counterparts, driven by an increase in k_{cat}^c (Table 3). This would lead to higher CO_2-saturated photosynthetic rates at

low temperatures in the polar populations compared with the cold-temperate populations. Similarly, when comparing populations belonging to the genus *Palmaria*, it was observed that the endemic Antarctic species *Palmaria decipiens* showed significantly higher k_{cat}^c and k_{cat}^c/K_c at 4 °C than the Arctic *Palmaria palmata* (Table 2), which might be related to the much longer cold-water history of Antarctica relative to the Arctic Ocean (Zacher *et al.*, 2011).

Despite these differences in Rubisco kinetics at 4 °C between polar and temperate populations, and considering their similar [Rubisco]/[TSP] values (Table 3), we suspect the existence of a higher Rubisco activation state in polar red and brown seaweeds in order to achieve the photosynthetic rates that have been measured in previous studies of the same species and locations (Thomas and Wiencke, 1991; Iñiguez *et al.*, 2016*a*, *b*; Olischläger *et al.*, 2017). Young *et al.* (2015) also suggested that Rubisco must be almost fully active in Antarctic diatoms, after comparison of its photosynthetic carbon fixation rates with Rubisco k_{cat}^c and quantity at low temperatures.

In contrast, the polar populations of the chlorophyte *A. arcta* showed no significant differences in k_{cat}^c/K_c at 4 °C compared with the temperate population, although a more than 2-fold increase in the [Rubisco]/[TSP] of both polar populations was observed (Table 3). These results are in agreement with those reported by Devos *et al.* (1998), who observed a similar 2-fold increase in the relative Rubisco content of two psychrophilic strains of the chlorophyte genus *Chloromonas* compared with their mesophilic counterparts, which might suggest different photosynthetic cold-adaptation responses between form IB and form ID Rubiscos.

The Arctic population of *Phycodrys rubens* did not show cold-adaptive traits compared with the cold-temperate population of this species, in terms of either Rubisco kinetics or [Rubisco]/[TSP]. As this species grows in the lower sublittoral, its photosynthetic rates should be constrained by the low irradiance reaching these depths and not by the maximum Rubisco carboxylation rate, probably leading to a lack of energetically expensive CCMs (Raven *et al.*, 2002*a*, *b*, 2014), as suggested by the CCM proxies (Table 4).

It is unsurprising that the $(K_c)^{25\ °C}/(K_c)^{4\ °C}$ ratio of polar Rubiscos was not lower (i.e. K_c less temperature dependent) than that of their cold-temperate counterparts (Table 3), as all Rubiscos, from either polar or temperate populations, showed increasing affinity for CO_2 at decreasing temperatures at the expense of a reduced catalytic activity, which facilitates the CO_2 saturation of the enzyme. Thus, assuming that carbon fixation might constrain photosynthesis in cold waters, polar environments should lead to a selection for higher k_{cat}^c Rubiscos instead of lower K_c. However, this assumption does not take into account biochemical processes other than Rubisco activity that can be affected by temperature, such as RuBP regeneration (Bernacchi *et al.*, 2003). Our results showed that the ratios $(k_{cat}^c)^{25\ °C}/(k_{cat}^c)^{4\ °C}$ and $(k_{cat}^c/K_c)^{25\ °C}/(k_{cat}^c/K_c)^{4\ °C}$ were significantly lower in the Arctic *S. latissima* compared with its cold-temperate counterpart, but not in the other polar versus temperate population comparisons, while the lowest values of $(k_{cat}^c)^{25\ °C}/(k_{cat}^c)^{4\ °C}$ within the Rhodophyta and Ochrophyta were obtained for the polar endemic species analyzed from each phylum (Table 2). This might reflect adaptation of the enzyme's temperature sensitivity according to its environment, as previously described (Sage, 2002; Galmés *et al.*, 2005, 2015, 2016; Young *et al.*, 2015).

Conclusions

Our results provide novel data on Rubisco kinetics from ecologically relevant polar and cold-temperate seaweeds belonging to different taxonomic groups. In contrast to previous findings in other photosynthetic groups, there was no correlation between either K_c or [Rubisco]/[TSP] and the CCM proxies for the red and brown seaweeds analyzed in the present study. Moreover, most of the analyzed polar populations showed signs of CCMs despite the lower K_c in form ID seaweed Rubiscos and the higher dissolved $[CO_2]$ in air-equilibrated seawater at 4 °C. We also report evidence of cold adaptation in Rubisco carboxylation kinetics or [Rubisco]/[TSP] of polar macroalgae likely possessing CCMs. In spite of this, photosynthesis at low temperatures and saturating irradiance conditions in red and brown seaweeds must be constrained by carbon fixation rates, and must require a high Rubisco activation state. Further studies of the regulation of form ID Rubiscos (see Mueller-Cajar *et al.*, 2011; Loganathan *et al.*, 2016) in seaweeds, about which data are currently scarce, are needed in order to make accurate predictions of productivity and ecosystem functioning in near-future scenarios.

Supplementary data

Supplementary data are available at *JXB* online.

Table S1. Rubisco carboxylation kinetics at 25°C taken from other datasets and used in Fig. 3.

Acknowledgements

This work was financed by projects CTM2011-24007/ANT and CGL2015-67014R, and also partially financed by projects AGL2009–07999 and AGL2013–42364R, from the Spanish Ministry for Science and Innovation and the Spanish Ministry for Economy and Competitiveness. CI was supported by an FPU grant from the Spanish Ministry for Education. Part of this work was performed at the International Arctic Environmental Research and Monitoring Facility, Ny-Ålesund, Spitsbergen, Norway. We thank Raquel Carmona and M. Rosario Lorenzo for their help taking the samples during the stay in Ny-Ålesund. We also thank the AWI diving team, Claudia Daniel, Andreas Wagner, and Inka Bartsch for providing us with the algal material. Furthermore, we thank Arantxa Molins for her help with the training for the Rubisco kinetic measurements, and Sergio Cañete and Elisa Gordo for supervising radioactivity handling.

References

Amsler CD, Rowley RJ, Laur DR, Quetin LB, Ross RM. 1995. Vertical distribution of Antarctic Peninsular macroalgae: cover, biomass, and species composition. Phycologia **34,** 424–430.

Andrews TJ, Lorimer GH. 1985. Catalytic properties of a hybrid between cyanobacterial large subunits and higher plant small subunits of ribulose bisphosphate carboxylase-oxygenase. Journal of Biological Chemistry **260,** 4632–4636.

Assali NE, Mache R, Loiseaux-de Goër S. 1990. Evidence for a composite phylogenetic origin of the plastid genome of the brown alga *Pylaiella littoralis* (L.) Kjellm. Plant Molecular Biology **15,** 307–315.

Badger MR, Andrews TJ, Whitney SM, Ludwig M, Yellowlees DC, Leggat W, Price GE. 1998. The diversity and co-evolution of Rubisco, plastids, pyrenoids, and chloroplast- based CO_2-concentrating mechanisms in algae. Canadian Journal of Botany **76,** 1052–1071.

Beardall J, Roberts S. 1999. Inorganic carbon acquisition by two Antarctic macroalgae, *Porphyra endivifolia* (Rhodophyta: Bangiales) and *Palmaria decipiens* (Rhodophyta: Palmariales). Polar Biology **21,** 310–315.

Beer S, Björk M, Beardall J. 2014. Photosynthesis in the marine environment. Oxford: Wiley-Blackwell.

Bernacchi CJ, Pimentel C, Long SP. 2003. In vivo temperature response functions of parameters required to model RuBP-limited photosynthesis. Plant, Cell and Environment **26,** 1419–1430.

Bischoff B, Wiencke C. 1993. Temperature requirements for growth and survival of macroalgae from Disko Island (Greenland). Helgoländer Meeresunters **47,** 167–191.

Bischoff B, Wiencke C. 1995. Temperature ecotypes and biogeography of Acrosiphoniales (Chlorophyta) with Arctic–Antarctic disjunct and Arctic/cold-temperate distributions. European Journal of Phycology **30,** 19–27.

Blayney MJ, Whitney SM, Beck JL. 2011. NanoESI mass spectrometry of Rubisco and Rubisco activase structures and their interactions with nucleotides and sugar phosphates. Journal of the American Society for Mass Spectrometry **22,** 1588–1601.

Boller AJ, Thomas PJ, Cavanaugh CM, Scott KM. 2015. Isotopic discrimination and kinetic parameters of RubisCO from the marine bloom-forming diatom, *Skeletonema costatum*. Geobiology **13,** 33–43.

Bolton JJ, Lüning K. 1982. Optimal growth and maximal survival temperatures of Atlantic *Laminaria* species (Phaeophyta) in culture. Marine Biology **66,** 89–94.

Boudreau BP. 1997. Diagenetic models and their implementation modelling transport and reactions in aquatic sediments. Berlin: Springer.

Bradford MM. 1976. A rapid and sensitive method for the quantitation of microgram quantities of protein utilizing the principle of protein-dye binding. Analytical Biochemistry **72,** 248–254.

Cavanagh AP, Kubien DS. 2014. Can phenotypic plasticity in Rubisco performance contribute to photosynthetic acclimation? Photosynthesis Research **119,** 203–214.

Davison IR. 1987. Adaptation of photosynthesis in *Laminaria saccharina* (Phaeophyta) to changes in growth temperature. Journal of Phycology **23,** 27.

Devos N, Ingouff M, Loppes R, Matagne R. 1998. RUBISCO adaptation to low temperatures: a comparative study in psychrophilic and mesophilic unicellular algae. Journal of Phycology **34,** 665–669.

Dunton KH, Schell DM. 1987. Dependence of consumers on macroalgal (*Laminaria solidungula*) carbon in an Arctic kelp community: $\delta^{13}C$ evidence. Marine Biology **93,** 615–625.

Egleston ES, Sabine CL, Morel FMM. 2010. Revelle revisited: buffer factors that quantify the response of ocean chemistry to changes in DIC and alkalinity. Global Biogeochemical Cycles **24,** GB1002.

Falkowski P, Schofield O, Katz M, Van de Schootbrugge B, Knoll A. 2004. Why is the land green and the ocean red? In: Thierstein H, Young J, eds. Coccolithophores. Berlin: Springer, 429–453.

Fortes MD, Lüning K. 1980. Growth rates of North Sea macroalgae in relation to temperature, irradiance and photoperiod. Helgoländer Meeresunters **34,** 15–29.

Galmés J, Flexas J, Keys AJ, Cifre J, Mitchell R, Madgwick P, Haslem R, Medrano H, Parry MA. 2005. Rubisco specificity factor tends to be larger in plant species from drier habitats and in species with persistent leaves. Plant, Cell and Environment **28,** 571–579.

Galmés J, Hermida-Carrera C, Laanisto L, Niinemets Ü. 2016. A compendium of temperature responses of Rubisco kinetic traits: variability among and within photosynthetic groups and impacts on photosynthesis modeling. Journal of Experimental Botany **67,** 5067–5091.

Galmés J, Kapralov MV, Andralojc PJ, Conesa MÀ, Keys AJ, Parry MA, Flexas J. 2014. Expanding knowledge of the Rubisco kinetics variability in plant species: environmental and evolutionary trends. Plant, Cell & Environment **37,** 1989–2001.

Galmés J, Kapralov MV, Copolovici LO, Hermida-Carrera C, Niinemets Ü. 2015. Temperature responses of the Rubisco maximum carboxylase activity across domains of life: phylogenetic signals, trade-offs, and importance for carbon gain. Photosynthesis Research **123,** 183–201.

Ghannoum O, Evans JR, Chow WS, Andrews TJ, Conroy JP, von Caemmerer S. 2005. Faster Rubisco is the key to superior nitrogen-use efficiency in NADP-malic enzyme relative to NAD-malic enzyme C_4 grasses. Plant Physiology **137,** 638–650.

Giordano M, Beardall J, Raven JA. 2005. CO_2 concentrating mechanisms in algae: mechanisms, environmental modulation, and evolution. Annual Review of Plant Biology **56,** 99–131.

Goldman JA, Kranz SA, Young JN, Tortell PD, Stanley RH, Bender ML, Morel FM. 2015. Gross and net production during the spring bloom along the Western Antarctic Peninsula. New Phytologist **205,** 182–191.

Gordillo FJ, Aguilera J, Jiménez C. 2006. The response of nutrient assimilation and biochemical composition of Arctic seaweeds to a nutrient input in summer. Journal of Experimental Botany **57,** 2661–2671.

Gordillo FJL, Carmona R, Viñegla B, Wiencke C, Jiménez C. 2016. Effects of simultaneous increase in temperature and ocean acidification on biochemical composition and photosynthetic performance of common macroalgae from Kongsfjorden (Svalbard). Polar Biology **39,** 1993–2007.

Hepburn CD, Pritchard DW, Cornwall CE, McLeod RJ, Beardall J, Raven JA, Hurd CL. 2011. Diversity of carbon use strategies in a kelp forest community: implications for a high CO_2 ocean. Global Change Biology **17,** 2488–2497.

Hermida-Carrera C, Kapralov MV, Galmés J. 2016. Rubisco catalytic properties and temperature response in crops. Plant Physiology **171,** 2549–2561.

Heureux AMC, Young JN, Whitney SM, Eason-Hubbard MR, Lee RBY, Sharwood RE, Rickaby REM. 2017. The role of Rubisco kinetics and pyrenoid morphology in shaping the CCM of haptophyte microalgae. Journal of Experimental Botany **68,** 3959–3969.

Holaday AS, Martindale W, Alred R, Brooks AL, Leegood RC. 1992. Changes in activities of enzymes of carbon metabolism in leaves during exposure of plants to low temperature. Plant Physiology **98,** 1105–1114.

Hop H, Wiencke C, Vögele B, Kovaltchouk NA. 2012. Species composition, zonation, and biomass of marine benthic macroalgae in Kongsfjorden, Svalbard. Botanica Marina **55,** 399–414.

Iken K, Quartino M, Barrera Oro E, Palermo J, Wiencke C, Brey T. 1998. Trophic relations between macroalgae and herbivores. Reports on Polar and Marine Research **299,** 258–262.

Iñiguez C, Carmona R, Lorenzo MR, Niell FX, Wiencke C, Gordillo FJL. 2016*a*. Increased CO_2 modifies the carbon balance and the photosynthetic yield of two common Arctic brown seaweeds: *Desmarestia aculeata* and *Alaria esculenta*. Polar Biology **39,** 1979–1991.

Iñiguez C, Carmona R, Lorenzo MR, Niell FX, Wiencke C, Gordillo FJL. 2016*b*. Increased temperature, rather than elevated CO_2, modulates the carbon assimilation of the Arctic kelps *Saccharina latissima* and *Laminaria solidungula*. Marine biology **163,** 248.

Israel A, Hophy M. 2002. Growth, photosynthetic properties and Rubisco activities and amounts of marine macroalgae grown under current and elevated seawater CO_2 concentrations. Global Change Biology **8,** 831–840.

Johnston AM. 1991. The acquisition of inorganic carbon by marine macroalgae. Canadian Journal of Botany **69,** 1123–1132.

Jordan DB, Ogren WL. 1984. The CO_2/O_2 specificity of ribulose-1,5-bisphosphate carboxylase/oxygenase. Planta **161,** 308–313.

Kapralov MV, Kubien DS, Andersson I, Filatov DA. 2011. Changes in Rubisco kinetics during the evolution of C_4 photosynthesis in *Flaveria* (Asteraceae) are associated with positive selection on genes encoding the enzyme. Molecular Biology and Evolution **28,** 1491–1503.

Klenell M, Snoeijs P, Pedersen M. 2004. Active carbon in *Laminaria digitata* and *L. saccharina* (Phaeophyta) is driven by a proton pump in the plasma membrane. Hydrobiologia **514,** 41–53.

Koch M, Bowes G, Ross C, Zhang XH. 2013. Climate change and ocean acidification effects on seagrasses and marine macroalgae. Global Change Biology **19,** 103–132.

Kubien DS, Brown C, Kane H. 2011. Quantifying the amount and activity of Rubisco in leaves. Methods in Molecular Biology **684,** 349–362.

Le Corguillé G, Pearson G, Valente M, *et al*. 2009. Plastid genomes of two brown algae, *Ectocarpus siliculosus* and *Fucus vesiculosus*: further insights on the evolution of red-algal derived plastids. BMC Evolutionary Biology **9,** 253.

Loganathan N, Tsaia YC, Mueller-Cajar O. 2016. Characterization of the heterooligomeric red-type rubisco activase from red algae. Proceedings of the National Academy of Sciences **113,** 14019–14024.

Lüning K. 1984. Temperature tolerance and biogeography of seaweeds: the marine algal flora of Helgoland (North Sea) as an example. Helgoländer Meeresunters **38,** 305–317.

Maberly SC, Raven JA, Johnston AM. 1992. Discrimination between ^{12}C and ^{13}C by marine plants. Oecologia **91,** 481–492.

Meyer M, Griffiths H. 2013. Origins and diversity of eukaryotic CO_2-concentrating mechanisms: lessons for the future. Journal of Experimental Botany **64,** 769–786.

Morita K, Hatanaka T, Misoo S, Fukayama H. 2014. Unusual small subunit that is not expressed in photosynthetic cells alters the catalytic properties of rubisco in rice. Plant Physiology **164,** 69–79.

Mueller-Cajar O, Whitney SM. 2008. Evolving improved *Synechococcus* Rubisco functional expression in *Escherichia coli*. The Biochemical Journal **414,** 205–214.

Mueller-Cajar O, Stotz M, Wendler P, Hartl FU, Bracher A, Hayer-Hartl M. 2011. Structure and function of the AAA+ protein CbbX, a red-type Rubisco activase. Nature **479,** 194–199.

Nisbet EG, Grassineau NV, Howe CJ, Abell PI, Regelous M, Nisbet RER. 2007. The age of RubisCO: the evolution of oxygenic photosynthesis. Geobiology **5,** 311–355.

Novaczek I, Lubbers GW, Breeman AM. 1990. Thermal ecotypes in amphi-Atlantic algae. I. Algae of Arctic to cold-temperate distribution (*Chaetomorpha melagonium*, *Devaleraea ramentacea* and *Phycodrys rubens*). Helgoländer Meeresunters **44,** 459–474.

Olischläger M, Iñiguez C, Gordillo FJ, Wiencke C. 2014. Biochemical composition of temperate and Arctic populations of *Saccharina latissima* after exposure to increased pCO_2 and temperature reveals ecotypic variation. Planta **240,** 1213–1224.

Olischläger M, Iñiguez C, Koch K, Wiencke C, Gordillo FJ. 2017. Increased pCO_2 and temperature reveal ecotypic differences in growth and photosynthetic performance of temperate and Arctic populations of *Saccharina latissima*. Planta **245,** 119–136.

Pearce FG. 2006. Catalytic by-product formation and ligand binding by ribulose bisphosphate carboxylases from different phylogenies. The Biochemical Journal **399,** 525–534.

Perdomo JA, Cavanagh AP, Kubien DS, Galmés J. 2015. Temperature dependence of in vitro Rubisco kinetics in species of *Flaveria* with different photosynthetic mechanisms. Photosynthesis Research **124,** 67–75.

Quartino ML, Boraso de Zaixso AL. 2008. Summer macroalgal biomass in Potter Cove, South Shetland Islands. Antarctica: its production and flux to the ecosystem. Polar Biology **31,** 281–294.

Raven JA, Ball LA, Beardall J, Giordano M, Maberly SC. 2005. Algae lacking carbon-concentrating mechanisms. Canadian Journal of Botany **83,** 879–890.

Raven JA, Beardall J. 2003. Carbon acquisition mechanisms of algae: carbon dioxide diffusion and carbon dioxide concentrating mechanisms. In: Larkum AW, Douglas SE, Raven JA, eds. Photosynthesis in algae. Advances in Photosynthesis and Respiration, Vol. 14. Dordrecht: Kluwer Academic Publishers, 225–244.

Raven JA, Beardall J, Giordano M. 2014. Energy costs of carbon dioxide concentrating mechanisms in aquatic organisms. Photosynthesis Research **121,** 111–124.

Raven JA, Falkowski PG. 1999. Oceanic sinks for CO_2. Plant, Cell and Environment **22,** 275–278.

Raven JA, Johnston AM, Kübler JE, *et al*. 2002*a*. Mechanistic interpretation of carbon isotope discrimination by marine macroalgae and seagrasses. Functional Plant Biology **29,** 335–78.

Raven JA, Johnston AM, Kübler JE, *et al*. 2002*b*. Seaweeds in cold seas: evolution and carbon acquisition. Annals of Botany **90,** 525–536.

Roeske CA, O'Leary MH. 1984. Carbon isotope effects on the enzyme-catalyzed carboxylation of ribulose bisphosphate. Biochemistry **23,** 6275–6284.

Ruuska S, Andrews T, Badger M, Hudson G, Laisk A, Price GD, von Caemmerer S. 1998. The interplay between limiting processes in C_3 photosynthesis studied by rapid-response gas exchange using transgenic tobacco impaired in photosynthesis. Australian Journal of Plant Physiology **25,** 859–870.

Sage RF. 2002. Variation in the k_{cat} of Rubisco in C_3 and C_4 plants and some implications for photosynthetic performance at high and low temperature. Journal of Experimental Botany **53,** 609–620.

Savir Y, Noor E, Milo R, Tlusty T. 2010. Cross-species analysis traces adaptation of Rubisco toward optimality in a low-dimensional landscape. Proceedings of the National Academy of Sciences, USA **107,** 3475–3480.

Seemann JR, Badger MR, Berry JA. 1984. Variations in the specific activity of ribulose-1,5-bisphosphate carboxylase between species utilizing differing photosynthetic pathways. Plant Physiology **74,** 791–794.

Sharkey TD, Berry JA. 1985. Carbon isotope fractionation of algae influenced by an inducible CO_2-concentrating mechanism. In: Lucas WJ, Berry JA, eds. Inorganic carbon uptake by aquatic photosynthetic organisms. Rockville: American Society of Plant Physiologists, 389–401.

Sharwood RE, Ghannoum O, Kapralov MV, Gunn LH, Whitney SM. 2016. Temperature responses of Rubisco from Paniceae grasses provide opportunities for improving C_3 photosynthesis. Nature Plants **2,** 16186.

Sharwood RE, von Caemmerer S, Maliga P, Whitney SM. 2008. The catalytic properties of hybrid Rubisco comprising tobacco small and sunflower large subunits mirror the kinetically equivalent source Rubiscos and can support tobacco growth. Plant Physiology **146,** 83–96.

Sherlock JA, Raven JA. 2001. Interactions between carbon dioxide and oxygen in the photosynthesis of three species of marine red algae. Botanical Journal of Scotland **113,** 301–307.

Skirrow G. 1975. The dissolved gases-carbon dioxide. In: Wiley JP, Skirrow G, eds. Chemical oceanography, **Vol. 2**. New York: Academic Press, 1–192.

Spreitzer RJ, Salvucci ME. 2002. Rubisco: structure, regulatory interactions, and possibilities for a better enzyme. Annual Review of Plant Biology **53,** 449–475.

Stepien CC. 2015. Impacts of geography, taxonomy and functional group on inorganic carbon use patterns in marine macrophytes. Journal of Ecology **103,** 1372–1383.

Surif MB, Raven JA. 1989. Exogenous inorganic carbon sources for photosynthesis in seawater of the Fucales and Laminariales (Phaeophyta): ecological and taxonomic implications. Oecologia **78,** 97–105.

Tabita FR, Satagopan S, Hanson TE, Kreel NE, Scott SS. 2008. Distinct form I, II, III, and IV Rubisco proteins from the three kingdoms of life provide clues about Rubisco evolution and structure/function relationships. Journal of Experimental Botany **59,** 1515–1524.

Tcherkez G. 2013. Modelling the reaction mechanism of ribulose-1,5-bisphosphate carboxylase/oxygenase and consequences for kinetic parameters. Plant, Cell & Environment **36,** 1586–1596.

Tcherkez GGB, Farquhar GD, Andrews TJ. 2006. Despite slow catalysis and confused substrate specificity, all ribulose bisphosphate carboxylases may be nearly perfectly optimized. Proceedings of the National Academy of Sciences, USA **103,** 7246–7251.

Thomas DN, Wiencke C. 1991. Photosynthesis, dark respiration and light independent carbon fixation of endemic Antarctic macroalgae. Polar Biology **11,** 329 –337.

tom Dieck I. 1992. North Pacific and North Atlantic digitate Laminaria species (Phaeophyta): hybridization experiments and temperature responses. Phycologia **31,** 147–163.

Valentin K, Zetsche K. 1989. The genes of both subunits of ribulose-1,5-bisphosphate carboxylase constitute an operon on the plastome of a red alga. Current Genetics **16,** 203–209.

van de Poll WH, Eggert E, Buma AGJ, Breeman AM. 2002. Temperature dependence of UV radiation effects in arctic and temperate isolates of three red macrophytes. European Journal of Phycology **37,** 59–68.

Wiencke C, Clayton MN, Gómez I, Iken K, Lüder UH, Amsler CD, Karsten U, Hanelt D, Bischof K, Dunton K. 2007. Life strategy, ecophysiology and ecology of seaweeds in polar waters. Reviews in Environmental Science and Biotechnology **6,** 95–126.

Wiencke C, tom Dieck I. 1989. Temperature requirements for growth and temperature tolerance of macroalgae endemic to the Antarctic region. Marine Ecology Progress Series **54,** 189–197.

Whitney SM, Baldet P, Hudson GS, Andrews TJ. 2001. Form I Rubiscos from non-green algae are expressed abundantly but not assembled in tobacco chloroplasts. The Plant Journal **26,** 535–547.

Whitney SM, Houtz RL, Alonso H. 2011. Advancing our understanding and capacity to engineer nature's CO_2-sequestering enzyme, Rubisco. Plant Physiology **155,** 27–35.

Yamori W, Noguchi K, Terashima I. 2005. Temperature acclimation of photosynthesis in spinach leaves: analyses of photosynthetic components and temperature dependencies of photosynthetic partial reactions. Plant, Cell and Environment **28,** 536–547.

Yeoh HH, Badger MR, Watson L. 1981. Variations in kinetic properties of ribulose-1,5-bisphosphate carboxylases among plants. Plant Physiology **67,** 1151–1155.

Young JN, Goldman JA, Kranz SA, Tortell PD, Morel FM. 2015. Slow carboxylation of Rubisco constrains the rate of carbon fixation during Antarctic phytoplankton blooms. New Phytologist **205,** 172–181.

Young JN, Heureux AM, Sharwood RE, Rickaby RE, Morel FM, Whitney SM. 2016. Large variation in the Rubisco kinetics of diatoms reveals diversity among their carbon-concentrating mechanisms. Journal of Experimental Botany **67,** 3445–3456.

Zacher K, Rautenberger R, Hanelt D, Wulff A, Wiencke C. 2011. The abiotic environment of polar benthic algae. In: Wiencke C, ed. Biology of polar benthic algae. Berlin: De Gruyter, 9–22.